Remote Powering Platform for Implantable Sensor Systems at 2.45 GHz

Onur Kazanc[1], Gurkan Yilmaz[1], Franco Maloberti[2], Catherine Dehollain[1]

[1] RFIC Group, Ecole Polytechnique Federale de Lausanne, Lausanne, Switzerland
[2] Integrated Microsystems Laboratory, University of Pavia, Pavia, Italy

***Abstract*— Far-field remotely powered sensor systems enable long distance operation for low-power sensor systems. In this work, we demonstrate a remote powering platform with a miniaturized antenna and remote powering base station operating at 2.45 GHz. The rectenna, which is the energy receiving and conversion element of the sensor system, is designed and measured. The measurements for the tag are performed within 15 cm distance from the remote powering base station. The realized gain of the tag antenna is measured as -3.3 dB, which is 0.5 dB close to the simulations, where simulated realized gain is -2.8 dB.**

I. Introduction

The development of RFIDs gives rise to the implementation of wireless sensor systems for remote monitoring and real-time wireless telemetry. One of the advantages of these systems is their battery-free operation which brings miniaturization. Likewise in RFID, remotely powered sensor systems utilize ISM frequency bands. For near-field inductive coupling, the operation frequency is generally selected as 13.56 MHz while for far-field electromagnetic coupling, 900 MHz and 2.45 GHz frequency bands are chosen [1]. The wireless sensor systems, which utilize near-field coupling, are mainly focusing on power levels greater than 200 μW [2]. The link efficiency of these systems suffers mainly because of lateral or angular misalignment between the transmitter and receiver coil [3].

Although, far-field electromagnetic coupling provide lower energy density compared to near field coupling, it can provide a wider coverage of area thanks to the antenna radiation pattern. Therefore, it ensures transmission of power not limited to the radiator area, and the power delivered is not affected by the horizontal misalignment of the receiving tag antenna. An application platform of remotely powered sensor system with electromagnetic coupling is presented in Figure 1. Note that, the beamwidth of the patch antenna can cover a mouse cage where animal mobility is expected.

We aim to design a remote powering platform for implantable sensor systems, where the receiving antenna is chosen to operate at 2.45 GHz. The chosen frequency at which the antenna exhibits relatively higher gain than 900 MHz thanks to its shorter wavelength. Therefore, it enables implantable systems with smaller device footprint.

Implanting a device inside the body requires certain specifications to be satisfied in order to guarantee that the body will accept the implant. Otherwise, the body exhibits foreign body reaction to the implant and it has to be removed. Amongst these specifications, two major goals have been considered in the scope of this study: biocompatibility and bidirectional diffusion barrier. A polymer based packaging is employed in order to protect the implant from the tissues and vice versa. Therefore, Polydimethylsiloxane (PDMS) is selected as the packaging material since it is shown to be biocompatible [4]. Moreover, it is preferred as a moisture barrier material thanks to its hydrophobicity [5].

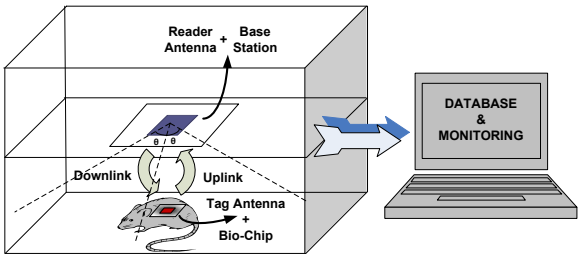

Fig. 1. Application platform to measure vital values of laboratory mouse.

In this work, we have developed a remote powering platform with base station and receiver rectenna, which is composed of the antenna and the rectifier, coated with PDMS polymer. In Section II the rectenna design, which includes rectifier and PDMS coated antenna, is presented. Section III describes the base station structure and its components. In Section IV patch antenna design and characterization are given. In Section V measurement results of the power link, which is characterized in air, are given. In Section VI results of this work are discussed.

II. Rectenna

A. Determining Non-Linear Rectifier Impedance

The impedance matching between receiving antenna and the rectifier determines how much of the incident power on the antenna is delivered to the rectifier. In order to maximize impedance matching, the input impedance of the rectifier should be determined accurately. Large signal s-parameter (LSSP) simulation permits obtaining the input impedance of a rectifier when it is matched to its source [6]. The simulation uses the the model of a commercially available diode used to build a bridge rectifier (Avago HSMS-2828) as shown in Fig. 2. The test circuit includes a single tone source at 2.45 GHz.

978-1-4244-7929-0/14/$26.00 ©2014 IEEE

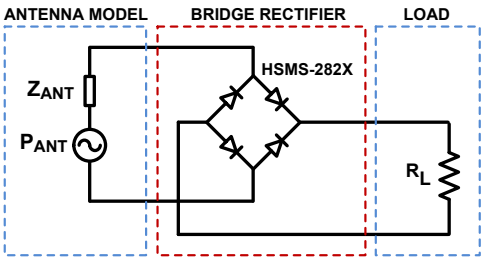

Fig. 2. Circuit schematic used to determine input impedance of the rectifier.

In order to estimate the input power for the LSSP simulation, initial antenna simulations and path loss calculations provide an expected input power of 3.6 dBm at the input of the rectifier. By using this power we have performed an LSSP simulation. In order to ensure that the source and rectifier impedances are matched for obtaining correct input impedance of the rectifier, we use the built-in optimizer of Agilent ADS. It minimizes the reflection coefficient between the source and the load and therefore maximizes impedance matching by finding the conjugate input impedance for the given input power. The resulting input impedance of the rectifier is found as $Z_{RECT} = 9.5 - j102\ \Omega$. We use the simulated input impedance of the rectifier to reach its complex conjugate impedance in the antenna design ($Z_{ANT} = 9.5 + j102\ \Omega$).

B. Antenna with Inductively Coupled Feed Loop

The layout of a planar meandered antenna with inductively coupled feed loop is shown in Fig. 3. It ensures maximum impedance matching thanks to its geometry which enables setting real and imaginary parts of the impedance independent of each other by tuning the spacing between the feed loop and the radiating body of the antenna [7].

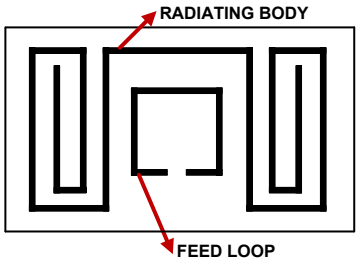

Fig. 3. Layout of tag antenna.

The real and imaginary parts of the antenna impedance $Z_{ANT} = R_{ANT} + jX_{ANT}$ are defined as;

$$R_{ANT} = \frac{(2\pi f M)^2}{R_{RB}} \qquad X_{ANT} = 2\pi f L_{loop} \tag{1}$$

where M is the mutual inductance between the radiating body of the antenna and the feed loop, L_{loop} is the inductance of the feed loop, and R_{RB} is the resistance of the radiating body of the antenna at its resonance frequency. Notice that the input resistance of the antenna depends on the mutual inductance M while input reactance is solely inductance of the feed loop L_{loop} itself.

C. Tag Antenna Design with Polymer Package

The packaging material affects the critical parameters of the implantable antenna such as input impedance and gain. Moreover, the thickness of the material is another design parameter which affects both antenna characteristics, especially in the near field, and barrier properties which determines the safe duration of the implant inside the body. The effect in the near field can be simply explained from the variation of electrical permittivity ($\epsilon_{r,air}$=1 and $\epsilon_{r,pdms}$= 2.3-2.8) in the vicinity of the antenna. In this work we used Sylgard-184 silicone elastomer from Dow Corning. It has a relative permittivity of $\epsilon_R = 2.68$ and a loss tangent of tanδ=0.0013.

The antenna is chosen to have a polymer package thickness of 8.5 mm in order to achieve reduced sensitivity to the thickness of the packaging. The simulation of the antenna targets for optimization of the input impedance for the conjugate matching with the rectifier ($Z_{ANT} = Z^*_{CHIP} = 9.5 + j102\ \Omega$). We have designed an antenna using Rogers 4003C substrate ($\epsilon_r = 3.55$) with loss tangent tanδ = 0.003 and having a thickness of 0.5 mm. The antenna is simulated using CST Microwave Studio for full-wave 3D simulations. Once the antenna is tuned for the desired input impedance, then the far-field radiation pattern is obtained by the simulator. In Fig. 4 the 3D radiation pattern of the tag antenna is depicted. It exhibits a maximum gain of -2.8 dB at 2.45 GHz.

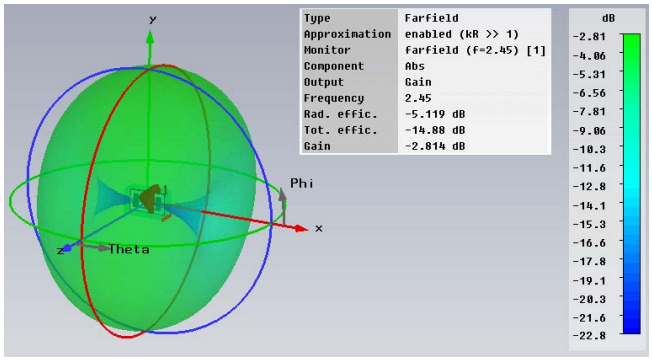

Fig. 4. 3D radiation pattern of the tag antenna.

D. Polymer Packaging

In order to coat the antenna evenly from each side, a mold has been designed using 0.8 mm FR4. Bottom plate of the mold is perforated such that the antenna fits into the mold leaving equal distances to the front and back border of the mold. Following Trimethlylchlorosilane (TMCS) treatment of the mold, which prevents sticking of PDMS and hence makes peeling easier; a Sylgard-184 solution is poured into the mold and cured for 2 hours at 80°C. PDMS solution

is composed of base agent and curing agent at a 10:1 ratio, respectively. Fig. 5 illustrates the alignment of the antenna to the molding structure. As previously mentioned the thickness of the antenna with PDMS coating is 8.5 mm. Therefore, the front and back thickness of PDMS (a) is 4 mm, sidewall thickness (b) is 1 mm, and the thickness of the antenna substrate (c) is 0.5 mm.

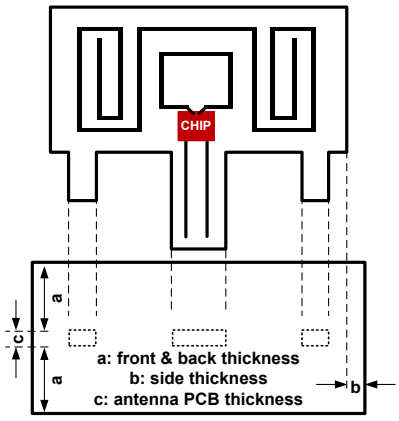

Fig. 5. Front view of the antenna and top view of the bottom plate of the mold.

In Fig. 6 the antenna with the mounted rectifier, which is coated with PDMS is shown. The final volume of the implantable rectenna is 18x11x8.5 mm^3. At the tail of the package the RC output load and terminals to measure DC output voltage of the rectifier are highlighted.

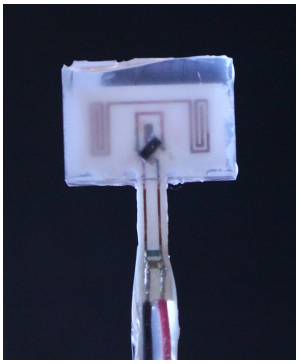

Fig. 6. Fabricated antenna with PDMS coating.

III. Remote Powering Base Station

The block diagram of the remote powering base station is shown in Fig. 7. The signal chain consists of a PLL frequency synthesizer (Analog Devices ADF4360-0) for carrier frequency generation and a power amplifier (RFMD 2172). The power amplifier is utilized to increase the output power of the base station sufficient for remote powering applications. The power amplifier, which is driven by the PLL, has 1 dB compression point at 23 dBm. The signal chain is completed by a transmitting patch antenna, where the output power of the power amplifier absorbed and radiated.

The PLL is programmable through the SPI port by using Texas Instruments MSP430 microcontroller. We have measured the output power of the base station while sweeping the output power of the PLL through the programmable SPI interface using the microcontroller. The output power of the remote powering base station ranges from +14.2 dBm to +23 dBm.

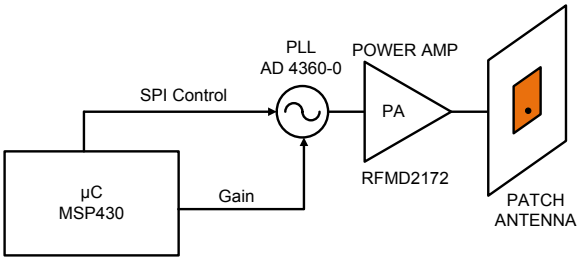

Fig. 7. Block diagram of remote powering base station for 2.45 GHz.

IV. Patch Antenna

Once the tag is fabricated, it is pre-measured with a wideband antenna, in this case a helical antenna, in order to find its resonance frequency before further characterization. The tag antenna, which is connected with rectifier and the output load, is measured and resonates at 2441 MHz. Next, the design and fabrication of patch antenna for 2441 MHz is performed once resonance of the tag antenna is measured.

The antenna of the remote powering base station is chosen as a patch antenna. The angle of emission is directed towards one direction and exhibits a beamwidth around 90°. This enables the antenna to be used for the proposed monitoring application. The implemented patch antenna of the RFID reader is based on an inset-fed patch antenna [8]. The antenna, which is designed for 2441 MHz, is built on a Rogers 5880 Duroid (ϵ_r=2.2) substrate with a low tangent loss (tanδ $\approx$ 0.005). The 3D full-wave simulation of the patch antenna is performed using CST Microwave Studio. The radiation pattern of the patch antenna is measured in an anechoic chamber. The simulated and measured radiation pattern is depicted in Fig. 8. The maximum gain of the patch antenna is measured as 7.2 dB while simulated maximum gain is 7.4 dB.

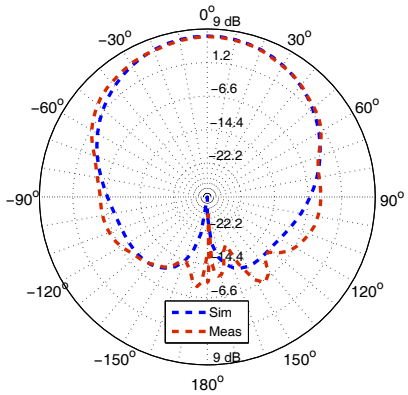

Fig. 8. Simulated and measured radiation pattern of the inset-fed patch antenna.

The fabricated patch antenna is measured with a vector network analyzer (VNA) in order to determine input reflection coefficient (S_{11}). The input reflection coefficient of the antenna is measured as -18 dB at 2441 MHz.

V. Measurement Results

We derive the realized gain $G_{RX(R)}$ of the tag antenna indirectly by simulating and measuring rectenna while knowing the path loss, output power of the remote powering base station, and the patch antenna gain. The measurement scheme of the rectenna is depicted in Fig. 9. The transmitting and receiving antennas are placed d =15 cm apart from each other in order to operate in far-field region.

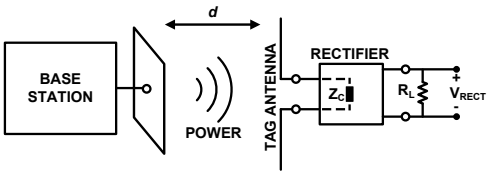

Fig. 9. Measurement setup for rectenna characterization.

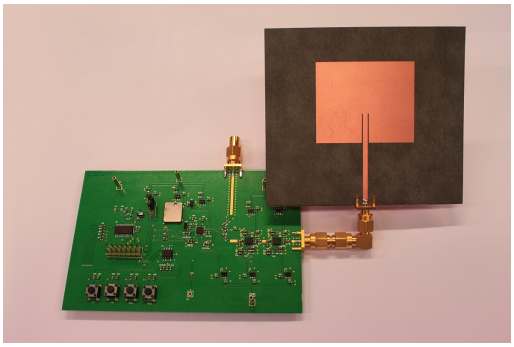

Fig. 10. Remote powering base station with patch antenna.

The P_{EIRP} of the remote powering base station shown in Fig. 10 is set to 30.2 dBm (≈1W). Then we calculate the path loss for 15 cm separation, which is found as 23.8 dB. Subtracting this from the P_{EIRP}, the expected input power for an isotropic radiator is 6.4 dBm and the expected power for our tag antenna, which has a simulated gain of -2.8 dB, is 3.6 dBm. Corresponding simulated efficiency of the rectifier for the given input power is found as 10.9% by using harmonic balance simulator. The realized gain of the tag antenna $G_{RX(R)}$ can be written by modified Friis equation,

$$G_{RX(R)} = \frac{P_{OUT}}{P_{TX} \cdot G_{TX} \cdot \left[\frac{\lambda}{4\pi d}\right]^2 \cdot \eta} \qquad (2)$$

where the efficiency of the rectifier (η) is accounted for. By measuring the rectenna with an output load of R_L= 30 kΩ we obtained a DC output voltage V_{RECT} equal to 2.6 V, whereas the simulated output voltage is 2.74 V assuming ideal matching. Measured and simulated output powers are 250 μW and 225 μW, respectively. Using (2) we calculate the realized gain $G_{RX(R)}$ of the tag antenna while assuming the rectifier efficiency is kept constant at 10.9 %. We calculated the realized gain of the tag antenna as -3.3 dB. Based on these results, we find the difference between the simulations and the measured realized gain $G_{RX(R)}$ as 0.5 dB. This difference can be explained by the nonideal impedance matching and efficiency variation in the rectifier. Nevertheless, the proposed method enables characterization of the remote powering link in a simple and accurate manner. Note that the measurement of the rectenna is performed in air and output power level is above 200 μW. In order to verify in-vivo performance, antenna is needed to be redesigned for in-vivo environment for realistic surroundings.

VI. Conclusion

In this work we have presented a remote powering platform targeting implantable sensor system applications at 2.45 GHz. The work covers the design of the remote powering base station and the receiving tag antenna with the rectifier. The tag antenna is coated with polymer and the employed molding method is described. Measurements are performed with the rectenna, which is composed of the designed tag antenna and a commercial rectifier in order to achieve real application measurements. The remote powering link is characterized from remote powering base station to the output of the rectifier. The measured antenna performs a realized gain of -3.3 dB while simulated realized gain is -2.8 dB, showing that measurements and simulations agree well.

Acknowledgment

This work is funded by Nano-Tera initiative of Swiss National Funding (SNF) project entitled “I-Ironic” and by SNF project entitled “Epilepsy in-vivo”.

References

[1] K. Finkenzeller, *“RFID Handbook: Fundamentals and Applications in Contactless Snart Cards and Identification"*, 2nd Edition, John Wiley & Sons, NY, USA, 2003

[2] N. Chaimanonart, D. J. Young, *“An Adaptively RF-Powered Wireless Batteryless In Vivo EKG and Core Body Temperature Sensing Microsystem for Untethered Genetically Engineered Mice Real-Time Monitoring”*, 6th International Conference on Network Sensing Systems (INSS), pp. 1-6, June 2009

[3] E.G. Kilinc, C. Dehollain; F. Maloberti, *“Design and optimization of inductive power transmission for implantable sensor system”*, XIth International Workshop on Symbolic and Numerical Methods, Modeling and Applications to Circuit Design (SM2ACD), 2010, pp.1-5, 4-6 Oct. 2010

[4] M. Belanger, Y. Marois, *“Hemocompatibility, Biocompatibility, Inflammatory and In-Vivo Studies of Primary Reference Materials Low-Density Polyethylene and Polydimethylsiloxane: A review."*, Journal of Biomedical Materials Research, vol.58, no.5, pp.467-477, Jul. 2001

[5] C. Lu, Y. Sun, S. J. Harley, E.A. Glascoe, *“Modeling Gas Transport and Reactions in Polydimethysiloxane"*, Proceedings in TOUGH Symposium, pp.1-8, Sep. 2012

[6] O. Kazanc, F. Maloberti, C. Dehollain, *“Simulation oriented rectenna design methodology for remote powering of wireless sensor systems"*, IEEE International Symposium on Circuits and Systems (ISCAS), pp.2877,2880, May 2012

[7] H. W. Son and C. S. Pyo, *“Design of RFID Tag Antennas Using an Inductively Coupled Feed"*, Electronics Letters, vol.41, no.8, pp.994-996, Sep. 2005

[8] C. A. Balanis, *“Antenna Theory: Analysis and Design”*, Second Edition, Wiley-Interscience, 2005